Submitted to Scripta Materialia in June 2003

Recoverable Stress Induced Martensitic Transformation in A Ferromagnetic CoNiAl Alloy

H. E. Karaca[1], Ibrahim Karaman[1]*, D.C. Lagoudas[2], H. J. Maier[3], Y.I. Chumlyakov[4]

[1]Department of Mechanical Engineering, Texas A&M University, College Station, TX 77843

[2]Department of Aerospace Engineering, Texas A&M University, College Station, TX 77843

[3]Lehrstuhl für Werkstoffkunde, University of Paderborn, 33095 Paderborn, Germany

[4] Siberian Physical-Technical Institute, Tomsk, 634050, Russia

*: Corresponding Author

ABSTRACT

The stress-induced martensitic transformation characteristics of a new CoNiAl alloy were investigated under compression. Pseudoelasticity, stages of transformation, temperature dependence of the pseudoelasticity and thermal cycling under constant stress were revealed. It is found that the present CoNiAl alloy is a candidate material not only for magnetic shape memory but also conventional and high-temperature shape memory alloy applications.

Keywords: Shape memory alloys; CoNiAl; Martensitic phase transformation; Ferromagnetic materials, Pseudoelasticity.

1. INTRODUCTION

In recent years, ferromagnetic shape memory alloys (FSMAs) have attracted increasing interest since Ullakko *et al.* [1] observed a large magnetic field induced strain (MFIS) in NiMnGa. Later Murray *et al.* [2] and Tickle and James [3] reported 6% and 4.3% MFIS respectively. Other FSMAs reported to date are FePd [4,5], FePt [6] and NiFeGa [7,8]. However, these materials are expensive and in most cases too brittle for practical applications. Similar to conventional shape memory alloys, FSMAs undergo martensitic phase transformation with the application of stress or by changing temperature. Main requirements to obtain large MFIS [9,10] are: 1) low twin boundary energy [9], 2) high strength matrix (to prevent dislocation slip), and 3) high microcrystalline anisotropy energy [10].

More recently, the potential of Co based alloys such as CoNiGa [11,12] and CoNiAl [12-15] as FSMAs have been revealed. CoNiAl alloys seem promising for FSMA applications because of the possibility for obtaining enough ductility for forming through thermal treatments

[16-18], relatively cheap constituents and the ability to control transformation temperatures and the Curie temperature (T_c) independently over a large composition range [13]. Upon cooling from the high-temperature cubic phase, CoNiAl alloys exhibit paramagnetic to ferromagnetic transition followed by thermoelastic martensitic transformation or vice versa, depending on their composition [13]. Although it has been shown [12-15] that CoNiAl alloys have the required magnetic characteristics to be potential FSMAs, the mechanical requirements have not been quantitatively investigated (first two requirements indicated above). Moreover, pseudoelastic behavior has not been revealed to date. SMAs with β parent phase such as CuNiAl and NiMnGa are known to have multiple martensite phases and intermartenistic transformations [19-22]. However, there has been no report on whether CoNiAl alloys exhibit multiple martensite phases. A through knowledge of martensitic transformation, transformation stress vs. strain behavior and transformation stress-temperature phase diagram of CoNiAl alloys is required to enhance the further development of these materials as FSMAs as well as establishing a basis for conventional shape memory applications of these alloys.

The aim of the present work is to address some of the above issues such as pseudoelastic response, the temperature dependence of martensitic transformation and transformation stress – temperature phase diagram of the Co-33Ni-29Al (in at. %) alloy. To the best of author's knowledge, this will be the first study of pseudoelasticity in these alloys.

II. EXPERIMENTAL PROCEDURE

A CoNiAl alloy has been obtained from Special Metals Corporation, New Hartford, NY. It was cast to a nominal composition of Co-32.9Ni-29.5 Al in atomic %. Specimens were homogenized at 1350 ° C for 24 hours in sealed quartz tubes and quenched in water. The resulting grain size was in the range of 1-10mm with no discernable grain boundary precipitates. Rectangular compression samples (4mm x 4mm x 8mm) were cut from the bulk material using electo-discharge machining. The transformation temperatures of the solution treated material were determined by a Perkin-Elmer Pyris-I differential scanning calorimeter (DSC) with a heating rate of 10 ºC/min. The martensite start (M_s) and finish (M_f) temperatures are -43 °C and -57 °C, respectively, while the austenite start (A_s) and austenite finish temperatures (A_f) were found to be -43 °C and -26 °C, respectively, as shown in Figure 1.

The mechanical experiments were conducted using an MTS servohydraulic test frame. The specimens were tested in the range of 25 °C to 170 °C to establish the Clausius–Clapeyron curve and to see how the pseudoelastic hysteresis changes with temperature. A miniature extensometer (3 mm gage) was used to measure the axial deformation during the experiments at temperatures as high as 100 °C. For higher temperatures, only crosshead-displacement measurement was used. The strain rate used was 5×10^{-4} s^{-1} to minimize rate effects and temperature rise during the experiments. The heating/cooling of the samples was achieved by conduction through compression plates heated using heating bands and cooled using liquid nitrogen flowing through copper tubing in contact with the plates. Temperature was measured using thermocouples spot-welded on the sample. The temperature variation on the samples during the experiments was ± 2°C.

The microstructure of the specimens was examined by optical microscopy (OM) and transmission electron microscopy (TEM). The OM specimens were etched in 75ml HCl, 75ml ethanol, 15g $CuSO_4$ and 10ml distilled water solution after mechanical polishing. For TEM, specimens were prepared by mechanical grinding and twin-jet electropolishing. The electropolishing solution consisted of 5% perchloric acid in ethanol, and large electron transparent areas were obtained when electropolishing was conducted at –15 °C. The resulting thin foils were examined in a PHILIPS CM 200 electron microscope operated at 200kV.

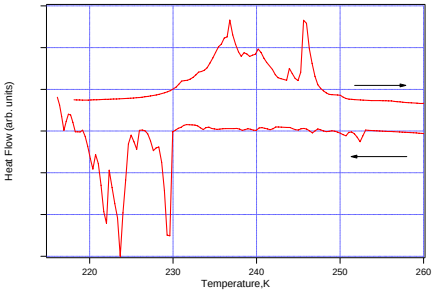

Figure 1: The differential scanning calorimetry results for the solutionized Co-33Ni-29Al.

III. RESULTS AND DISCUSSIONS

Figures 2.a,b and c show optical micrographs of the surface relief during cooling of the present alloy. The martensite lamella pattern appears in different grains. Figure 2.d illustrates the tweed-like pattern observed in the TEM prior to the transformation indicating a precursor phenomenon which is typical for FSMAs [23]. This precursor phenomena was interpreted as the existence of

an intermediate phase that form upon the volume increase of the lattice cell of the initial cubic phase [24].

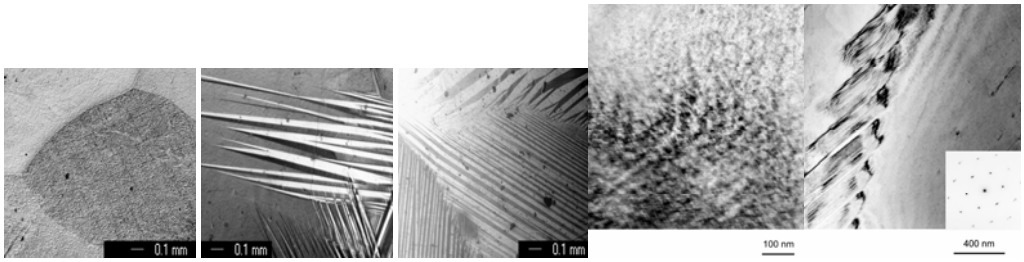

(a) (b) (c) (d) (e)

Figure 2: Optical micrographs of the surface relief of the CoNiAl alloy during cooling ((a), (b), (c)). The TEM bright field image in (d) shows a tweed-like contrast just above M_s which is an indication of a precursor phenomenon [23,24]. (e) shows the subplates of internally twinned residual martensite after loading to 6% and unloading (See Figure 3.a).

The results shown in Figure 3 are typical of the pseudoelastic compressive stress-strain curves obtained upon incremental deformation of conventional shape memory alloys above the A_f temperature. The narrow stress hysteresis upon unloading is similar to the one observed in CuNiAl as opposed to the wide hysteresis typical for NiTi based SMAs. The recoverable strains are superimposed on the compressive stress-strain curves with symbols in the figure. The critical stress for the nucleation of stress-induced martensitic transformation (SIM) is about 200 MPa while the maximum pseudoelastic strain is about 4%. The response is initially elastic followed by transformation of austenite (B2 phase) to martensite phases. As the material is deformed further at the end of the plateau region, the response is virtually elastic with martensite deforming in an elastic manner. The second elastic loading is followed by another low strain hardening region which could be either yielding of martensite or another phase transformation stage, or both. The stress level for the onset of dislocation slip is quite high (~1100 MPa) showing the high resistance of the matrix against dislocation slip which is desired for MFIS.

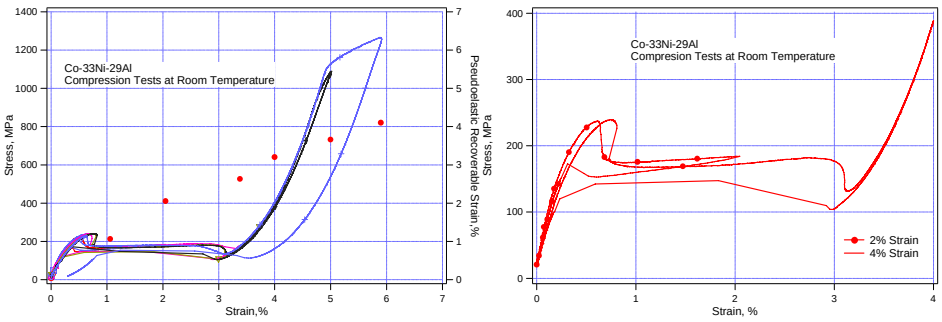

(a) (b)

Figure 3: (a) Compressive stress-strain response and recoverable strains of Co-33Ni-29Al as obtained in an incremental strain test. (b) shows the details of the tests unloaded at the 2 and 4% strain levels.

There are some notable features in Figure 3.a such as a significant stress drop after deformation starts, a plateau-like strain and another significant stress drop at the end of the plateau region. The stress drop at the beginning of the deformation is the indication of a significant difference between the nucleation stress of martensite and the stress required for phase front motion. At the end of the plateau region, it is expected that the transformation would end and elastic deformation of martensite would start. It is speculated that the second stress drop may be because of the formation of another phase front. The formation of a new phase front can be either because of the nucleation of a new martensite variant away from the previous one or because of a new phase transformation. Our argument is that the latter is more plausible and some direct and indirect evidences will be presented below. During unloading, the exact loading curve is followed until 3% strain and a stress increase occurs followed by a plateau-like strain and final elastic unloading. Note that the unloading conducted under the force control mode of the test frame, and thus, the entire unloading plateau region of the sample strained to 6% lasted only 0.4 seconds.

After nucleation of martensite upon loading, the stress for phase propagation is decreased by 70 MPa and kept constant up to 3% transformation strain whereas during unloading the stress needed for nucleation is 40 MPa lower than the stress required for the propagation of back transformation front. The stress hysteresis between the plateau regions is about 20-25MPa which is very low when compared to NiTi. Low stress hysteresis provides great advantage in actuator

and heat engine applications. High strength for slip, low stress hysteresis, high pseudoelastic strain at room temperature can make CoNiAl a new FSMA that also can be used as a conventional SMA.

The small irrecoverable strain after 6% straining is due to the residual martensite as shown by the TEM image in Figure 2.e. However, this residual martensite seems different from the stress or thermally induced martensite usually observed in typical SMAs such as NiTi and CuNiAl. There are subplates of internally twinned martensite which is usually observed in Fe-Ni alloys [25]. This martensite morphology was attributed to the formation of group of dispersed subplates as multiple nuclei [25]. The habit plane is clear in the figure, however, internal twins are not continuous and are somewhat wavy (Figure 2.e). The reason for the waviness is not clear at this point, however, Kishi *et al.* [23] argued that elastic, magnetic, and magnetoelastic energies control the structure of these boundaries.

Under the application of stress, it is virtually impossible to distinguish, based only on the compressive stress-strain curve, a two/or more stage transformation. A similar behavior was observed in NiTiCu single crystals under compression in which only one stress plateau existed although the transformation was a two stage one (B2→B19→B19') as demonstrated by thermal cycling under stress and TEM [26,27]. If the individual curves in Figure 3.a are compared with each other in detail, it is possible to see some significant differences as shown in Figure 3.b. Upon unloading at 2%, there is no stress drop which means that back transformation starts immediately after unloading starts. The stress hysteresis is extremely narrow. During loading to 4%, a second stress drop occurs at around 3% strain, which is attributed to a new phase transformation. The phase transformation continues after the second stress drop as the recoverable strains increases with increasing strain (Figure 3.a). Upon unloading at 4% strain, a stress jump occurs for the start of back transformation as opposed to the 2% unloading case. Note that there is a significant difference between the hysteresis loops of the 2% and 4% cases which can also be attributed to a two stage martensitic transformation. Two-stage phase transformation is also evident from the DSC results shown in Figure 1 in which two DSC peaks are observed both during cooling and heating. In NiMnGa [20-22] and Cu-based SMAs [19], multiple martensitic phases can form during deformation as well as in NiAl alloys [28,29]. However, the phases that form and the sequence of the nucleation of the phases are orientation and temperature dependent [19]. An intensive investigation on the single crystals of CoNiAl is

underway to reveal the orientation and temperature dependence of the thermoelastic martensitic transformation in CoNiAl alloys.

Another evidence for the two stage martensitic transformation is provided by the thermal cycling experiments conducted under external stress. Figure 4 presents the strain vs. temperature response of the present material at two different stress levels (100 and 200 MPa). Some of the observations are: (a) the transformation occurs in two stages, (b) the transformation temperatures are stress dependent, but the onset of lower temperature transformation is more temperature sensitive than the onset of higher temperature transformation, (c) the back transformation occurs in only one stage, (d) the transformation strain is about 4% which is in agreement with the compression experiments at room temperature (Figure 3.a), and (e) temperature hysteresis increases with increasing stress. Note that 200 MPa constant stress leads to almost one step forward transformation elucidating why the two stage deformation at room temperature compression experiments was not evident.

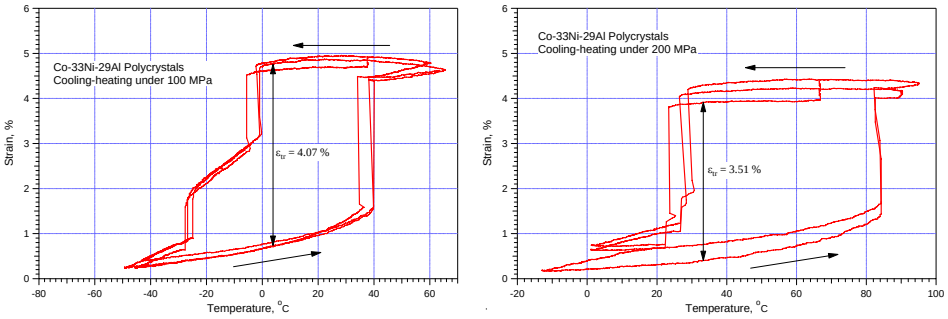

(a) (b)

Figure 4: Compressive strain vs. temperature response of Co-33Ni-29Al under constant stress, (a) under 100 MPa and (b) under 200 MPa.

In order to determine the effect of temperature on pseudoelastic behavior, compression experiments at different temperatures were conducted and the results are shown in Figure 5. A perfect pseudoelastic behavior with a large pseudoelastic temperature window (>160˚ C) is obtained at all temperatures. The x-axis of Figure 5 is represented in displacement as it was not possible to use the miniature extensometer above 100 °C. The strain measurement at room temperature resulted in 4% strain. There is no stress drop during loading although there is still a stress jump during unloading for the back transformation. The difference between the shapes of

the initial part of the stress-strain responses of different samples (Figs. 3 and 5) is attributed to the different texture of the individual samples because of the large grain size. It is well-known that martensitic transformation and shape memory response are strongly dependent on the orientation [30,31]. Moreover, two stage transformation is evident on the curves up to 130 °C. Above 130 °C, it is no longer possible to distinguish the two stages or one of the stages vanishes. The stress hysteresis increases from 30 MPa at room temperature to 80 MPa at 130 ° C. Then it decreases to 50 MPa at 150 °C and 170 °C.

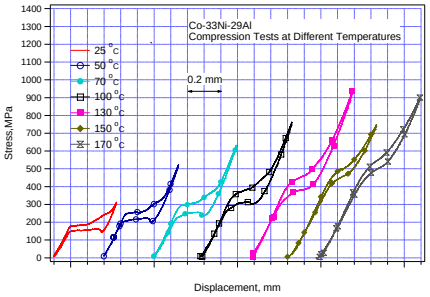

Figure 5: Compressive stress vs. displacement response of Co-33Ni-29Al at different temperatures.

The results in Figure 5 were used to construct the critical stress for martensitic transformation vs. temperature curve as shown in Figure 6. The values for both forward (M_s) and backward (A_s) transformation are included in the figure. It is evident that the trend satisfies the Clausius-Clapeyron (CC) relation. The CC slope is 2.47 MPa/K for loading. Through extrapolation of this data, the M_s temperature is obtained as –50 ° C under zero load which is in between the M_s and M_f temperatures obtained from the DSC results (Figure 1). The CC slope is significantly lower than what is observed in NiTi. This confirms that the pseudoelastic window for CoNiAl is significantly larger than in NiTi alloys even if they would have the same critical stress for slip. This can make CoNiAl a candidate material for high temperature SMA applications as well.

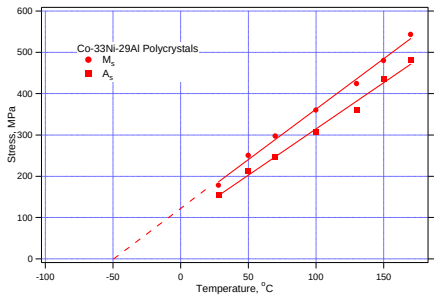

Figure 6: The critical stress for the onset of martensitic transformation as a function of temperature.

IV. CONCLUSIONS

In the present work, the salient features of the recoverable stress-induced martensitic transformation in Co-33Ni-29Al was investigated. The purpose was to reveal the ease of twin boundary motion, stress for dislocation slip and pseudoelastic characteristics that are needed for materials displaying high magnetic field induced strains. It was found that:

(1) After homogenization treatment, cast Co-33Ni-29Al demonstrates up to 4% pseudoelastic strain with a narrow stress hysteresis of 20-25 MPa at room temperature. An extended plateau region was observed with the martensite nucleation stress being significantly larger than the propagation stress. This is an indication of the low twin boundary energy which is a necessary condition for magnetic field induced strains.

(2) Perfect pseudoelasticity up to 170° C was shown. A pseudoelastic temperature window of more than 160° C is obtained which is significantly larger than in NiTi alloys making CoNiAl a candidate for high-temperature SMA applications.

(3) The slope of the Clausius-Clapeyron curve obtained for the stress-induced martensitic transformation is in the 2-3MPa / ° C range.

(4) A two stage phase transformation was revealed, and the stress required for the onset of dislocation slip is as high as 1100 MPa leading to a 900 MPa stress differential between stress-induced martensitic transformation and dislocation motion. This is also a necessary condition for obtaining large magnetic field induced strains.

Deleted: (1)

Formatted: Bullets and Numbering

Deleted: (2)

Deleted: (3)

Deleted: (4)

ACKNOWLEDGEMENTS

This work was supported by Army Research Office, Contract No. DAAD 19-02-1-0261.

REFERENCES:

1. K. Ullakko, J.K. Huang, C. Kantner, V.V. Kokorin and R.C. O'Handley, *Appl. Phys. Lett.*, 1996, vol. 69, p. 1966.
2. S. J. Murray, M. Marioni, P. G. Tello, S. M. Allen and R. C. O'Handley, *J. Magn. Magn. Mater.*, 2001, vol. 226, p. 945.
3. R. Tickle, R.D. James, *J. Magn. Magn. Mater.*, 1999, vol. 195, p. 627.
4. S. Muto, R. Oshima, and F.E. Fujita, *Scripta Metall.*, 1987, vol. 21, p. 465.
5. R.D. James, M. Wuttig, *Phil. Mag. A*, 1998, vol. 77, p. 1273.
6. T. Kakeshita, T. Takeuchi, T. Fukuda, T. Saburi, R. Oshima, S. Muto, and K. Kishio, *Mater. T. JIM*, 2000, vol. 41, p. 882.
7. K. Oikawa, T. Ota, Y. Sutou, T. Ohmori, R. Kainuma, and K. Ishida, *Mater. Trans. JIM*, 2002, vol. 43, p. 2360.
8. K. Oikawa, T. Ota, T. Ohmori, Y. Tanaka, H. Morito, A. Fujita, R. Kainuma, K. Fukamichi, and K. Ishida, *Appl. Phys. Lett.*, 2002, vol. 81, p. 5201.
9. T. Kakeshita T, K. Ullakko, *MRS Bull*., 2002, vol. 27, p. 105.
10. A. Vassiliev, *J Magn. Magn Mater*., 2002, vol. 242, p. 66.
11. M. Wuttig, J. Li and C. Craciunescu, *Scripta Mater.*, 2001, vol. 44, p. 2393.
12. K. Oikawa, T. Ota, F. Gejima, T. Ohmori, R. Kainuma, and K. Ishida, *Mater Trans*, 2001, vol. 42, p. 2472.
13. K. Oikawa, L. Wulff, T. Iijima, F. Gejima, T. Ohmori, A. Fujita, K. Fukamichi, R. Kainuma, and K. Ishida, *Appl. Phys. Lett*., 2001, vol. 79, p. 3290.
14. Y. Murakami, D. Shindo, K. Oikawa, R. Kainuma, and K. Ishida, *Acta Mater*. 2002, vol. 50, p. 2173.
15. H. Morito, A. Fujita, K. Fukamichi, R. Kainuma, K. Ishida, and K. Oikawa, *Appl. Phys. Lett*., 2002, vol. 81, p.1657.
16. R. Kainuma, M. Ise, C.C. Jia, H. Ohtani, and K. Ishida, *Intermetallics*, 1996, vol. 4, p.151.
17. K. Ishida, R. Kainuma, N. Ueno, and T. Nishizawa, *Metall. Trans. A*, 1991, vol. 22, p. 441.
18. K. Enami, S. Menno, *Met. Trans*., 1971, vol. 2, p. 1487.
19. K. Otsuka, H. Sakamato, and K. Shimizu, *Acta Metall.*, 1979, vol. 27, p. 585.

20. V.A. Chernenko, V.V. Kokorin, O.M. Babii, and I.K. Zasimchuk, *Intermetallics*, 1998, vol. 6, p. 29.
21. V.V. Martynov, V.V. Kokorin, *J. De Physique III*, 1992, vol. 2 , p.739.
22. V.A. Chernenko, V. L'vov, J. Pons, and E. Cesari, *J. Appl. Phys*., 2003, vol. 93, p. 2394.
23. Y. Kishi, C. Craciunescu, M. Sato, T. Okazaki, Y. Furuya, and M. Wuttig, *J. Magnestism Mag. Mater*., 2003, vol. 262, p. L186.
24. V.V. Kokorin, V.A. Chernenko, E. Cesari, J. Pons, and C. Segui, *J. Phys.: Condens. Matter*, 1996, vol. 8, p. 6457.
25. P.G. McDougal and C.M. Wayman, in *Martensite* Ed. By G.B. Olson and W.S. Owen, ASM Int., 1992.
26. H. Sehitoglu, I. Karaman, X. Zhang, A. Viswanath, Y. Chumlyakov, and H.J. Maier, *Acta Mater*., 2001, vol. 49, p. 3621.
27. H. Sehitoglu, I. Karaman, X. Zhang, H. Kim, Y. Chumlyakov, H.J Maier and I. Kireeva, *Metall. Mater. Trans. A*, 2001, vol. 32, p. 477.
28. D. Schryvers, P. Boullay, P.L. Potapov, R.V. Kohn, and J.M. Ball, *Int. J. Solids Struct*.,2002, vol. 39, p. 3543.
29. D. Schryvers, L.E. Tanner, *Ultramicroscopy*, 1990, vol. 32, p. 241.
30. H. Sehitoglu, I. Karaman, R. Anderson, X. Zhang, K. Gall, H.J. Maier, and Y. Chumlyakov, *Acta Mater*., 2000, vol. 48, p. 3311.
31. K. Gall, H. Sehitoglu, R. Anderson, I. Karaman, Y. Chumlyakov and I.V. Kireeva, *Mater. Sci. Eng. A*, 2001, vol. 317, p. 85.